Recombination of dyons into calorons in $SU(2)$ lattice fields at low temperatures

E.-M. Ilgenfritz and M. Müller-Preussker
Humboldt-Universität zu Berlin, Institut für Physik, Newtonstr. 15, D-12489 Berlin, Germany

B. V. Martemyanov and A. I. Veselov
Institute for Theoretical and Experimental Physics, B. Cheremushkinskaya 25, 117259 Moscow, Russia
(Received 12 February 2004; published 25 June 2004)

By cooling of equilibrium lattice fields at finite temperature in $SU(2)$ gauge theory it has been shown that topological objects (calorons) observed on the lattice in the confined phase possess a dyonic substructure which becomes visible under certain circumstances. Here we show that with the increasing temporal lattice extent the distribution in the caloron parameter space is modified such that the calorons appear nondissociated into constituent dyons. Still the calorons have nontrivial holonomy which is demonstrated by the Polyakov line behavior for these configurations. At vanishing temperature (on a symmetric lattice) topological lumps obtained by cooling show rotational symmetry in 4D for the action density, but a characteristic internal double-peak structure of Polyakov lines with respect to all (temporal and spatial) directions.

DOI: 10.1103/PhysRevD.69.114505 PACS number(s): 11.15.Ha, 11.10.Wx, 12.38.Lg, 14.80.Hv

I. INTRODUCTION

At high temperatures, near but below the deconfinement temperature, classical solutions of Yang-Mills equations with nontrivial holonomy [Kraan–van Baal (KvB) calorons [1,2]] are seen on the lattice for $SU(2)$ gauge theory to be frequently dissociated into dyons [3–6]. This means that the distance between the dyons forming a caloron,

$$d = \frac{\pi\rho^2}{b}, \tag{1}$$

is larger than the size of dyons (which is b/π for the case of maximally nontrivial holonomy). Here ρ is the instanton size parameter and b is the temporal periodicity interval.

These observations have been made by the use of cooling. Therefore, the question arises why such a substructure has not been observed by previous authors who have used the cooling method. In this paper we will argue that there is only a certain window of temperature or space-time asymmetry where it can be revealed by this method.

The interest in the existence of caloron constituents has increased since it has been demonstrated in Ref. [7] that a constituent substructure very reminiscent of the caloron solutions can also be identified without cooling, above and below the phase transition. This can be achieved by using the localization properties of the fermionic zero modes of a suitably chirally improved Dirac operator. The similarity with the properties of a caloron solution is strikingly realized for a certain fraction of configurations with topological charge $Q = \pm 1$, where the single zero mode is seen to change its localization when the periodicity of fermionic boundary conditions becomes modified. A systematic study [7] of the typical pattern of localization and delocalization followed by jumps of the zero mode has revealed that this pattern depends on the timelike holonomy exactly in a caloronlike way. Whereas the topological density has a much more complicated structure, the positions where the zero mode is pinned down actually show the signatures expected for caloron constituents [8]: they are local maxima of the topological density $q(x)$ with a sign as required by the chirality of the mode. This suggests that (dissociated or nondissociated) calorons might really form the semiclassical background of the gauge field near the phase transition.

Coming back to $SU(2)$ calorons with their two constituents, it seems that the quantities d and ρ appearing in Eq. (1) are impossible to be measured simultaneously: when d is seen by observation of separate dyon positions no instanton-like profile (of topological density) is observed which could be used to define ρ. When d goes to zero ($d \ll b$) an instanton size parameter ρ *can be measured* by comparison with the instanton's action density profile, but then *no dyons are seen* as separate objects. More precisely, the parameter d cannot be measured for *all* caloron configurations as the distance between constituents as long as only the action or topological charge densities are available as local observables to describe them.

The time periodicity parameter b defines the temperature T: $b = 1/T$. In order to demonstrate how the recombination of constituents depends on the temperature we can change the temporal extent b of the lattice.

We employ the standard relaxation cooling technique using the Wilson lattice action and concentrate on the investigation of lowest-action field configurations with $Q = \pm 1$. Besides the fact that solutions with $|Q| = 1$ are nonexistent on a torus in a mathematically strict sense [9], also the cooling method has a limited relevance. It cannot be used for revealing the full topological structure of the QCD vacuum even if the latter is semiclassical to a certain extent. In particular, it considerably weakens the chiral condensate compared with its value for equilibrium fields [10]. Moreover, it is well known that the Wilson action depends on the instanton (or caloron) scale size. Therefore, its minimization shrinks the localized solutions until they disappear "through the lattice meshs." Thus, small excitations will be lost first. In the literature—besides fermionic methods—there are better techniques like improved cooling, smoothing, smearing, etc., allowing us to decipher the topological long-range

structure of the gauge fields. But this task is *not* our concern in this paper. Here we ask the more modest question as to what kinds of simple classical solutions can be found from equilibrium gauge fields at different temperatures by successively minimizing the action.

This question remains interesting for those who want to build or apply semiclassical-like approximations—i.e., models like the instanton gas or liquid model [11] being successful in many phenomenological applications for which chiral symmetry breaking (and not quark confinement) is playing the major role [12]. Until now most of the cooling (or smoothing) results obtained at $T<T_c$ have been interpreted in terms of Belavin-Polyakov-Schwarz-Tyupkin (BPST) instanton [13] and Harrington-Shepard (HS) caloron [14] solutions, respectively, all exhibiting trivial asymptotic holonomy. Here we would like to convince the reader that the simplest caloron or instanton solutions seen after cooling have typically nontrivial holonomy, irrespectively of their possible dissociation into dyons pairs. Therefore, they cannot be correctly interpreted as BPST or HS solutions.

The paper is organized as follows. In Sec. II we draw the attention to the static nature of configurations near the deconfining transition. Section III presents our results on semiclassical configurations at finite temperatures, pointing out the loss of ''staticity'' and the increasing importance of the Polyakov loop for detecting the nontrivial substructure at lower temperature. In Sec. IV we extend the cooling studies to the symmetric torus. We emphasize that the KvB caloron solutions were constructed in an infinite spatial volume. When used at finite volume considerable deviations are to be expected when the spatial box size is no longer large compared to b, since the typical size of the constituents is b/π. Finally, in Sec. V, we discuss the consequences, also in the perspective of a twin paper by Gattringer *et al.* [15].

II. NONSTATICITY AND SEPARATION INTO CONSTITUENTS

It turns out that the possibility to observe the dyonic constituents of a KvB caloron as lumps of action depends on $(\pi\rho/b)^2$. In $SU(2)$ lattice gauge theory (LGT) at $\beta\equiv 4/g_0^2 = 2.2$ on a lattice $16^3\times 4$ the parameter ρ is concentrated near the value $\rho\approx 2.5a$ (a is the lattice spacing) [4]. With $b=4a$,

$$\left(\frac{\pi\rho}{b}\right)^2 \approx 4 \gg 1.$$

This means that dyons are well separated. The value of ρ in [4] was determined by fitting the lattice caloron with the analytic KvB caloron, and formula (1) was used. On the lattice $16^3\times 6$ (with $b=6a$) and at the same $\beta=2.2$ (i.e., at a temperature 1.5 times lower) the parameter $(\pi\rho/b)^2$ would be of the order $O(1)$. Then, from this simple arithmetics, one would expect that calorons are not dissociated into dyonic lumps anymore.

The possibility to measure the distance between dyons inside a caloron just by detecting the peaks of the action density on the lattice is given only in the case of well-separated objects. Indirectly this distance can be measured by measuring a quantity that can be called nonstaticity.[1] Unfortunately, cooling yields metastable plateaus only for temperatures below the deconfining temperature. On the other hand, this allows us to restrict ourselves in the following to *maximally nontrivial holonomy* because the average Polyakov line vanishes. To describe for this special case the relation between distance d and nonstaticity, we have considered analytical caloron solutions in continuous space-time. We divided the time interval b into N_t time slices and expressed the action in the ith time slice, $S_i=\Sigma_{\vec{x}} s_{\vec{x},i}$, in terms of the local action density $s_{\vec{x},i}$. The nonstaticity δ_t is defined as

$$\delta_t = \frac{\sum_{i=1}^{N_t}\sum_{\vec{x}} |s_{\vec{x},i+1}-s_{\vec{x},i}|}{\sum_{i=1}^{N_t}\sum_{\vec{x}} s_{\vec{x},i}}. \tag{2}$$

Obviously, this definition depends on the number of time slices, N_t, such that one would have $\delta_t\to 0$ for $N_t\to\infty$. In order to get an asymptotically N_t-independent quantity we will modify the definition of δ_t as follows:

$$\delta_t = \frac{\sum_{i=1}^{N_t}\sum_{\vec{x}} |s_{\vec{x},i+1}-s_{\vec{x},i}|}{\sum_{i=1}^{N_t}\sum_{\vec{x}} s_{\vec{x},i}} \frac{N_t}{4}. \tag{3}$$

The factor 1/4 has been chosen such that for a lattice $16^3\times 4$, where all the simulations were initially done using Eq. (2), the two definitions (3) and (2) agree.

With the definition (3) at hand we can calculate the nonstaticity of an analytic KvB caloron. The nonstaticity depends on the holonomy and on the distance between the constituents inside the caloron. For maximally nontrivial holonomy (which coincides with the average holonomy in the confinement phase) the constituent dyons have equal mass. For this simplified case we have determined a bifurcation value of the nonstaticity, $\delta_t^*=0.27$, choosing the distance between the constituents such that the two lumps of the action density (dyons) merge into one lump of the action density. This single lump is what we call a ''recombined caloron.'' As already mentioned, the nonstaticity uses the discreteness of a lattice configuration. The value δ_t^* is obtained by inserting the analytic form of the action density of a continuum KvB caloron solution [1], calculated exactly at the point of bifurcation, into the evaluation of Eq. (3) using a grid with lattice spacing $a=b/N_t$. In order to see how well defined at finite N_t this ''bifurcation value'' δ_t^* can be, we have evaluated it for various (even and odd) $N_t\geqslant 4$. The function $\delta_t^*(N_t)$ that goes to $\delta_t^*=0.27$ for $N_t\to\infty$ is presented in Fig. 1.

[1]See Ref. [6] where it has been defined in a slightly different way.

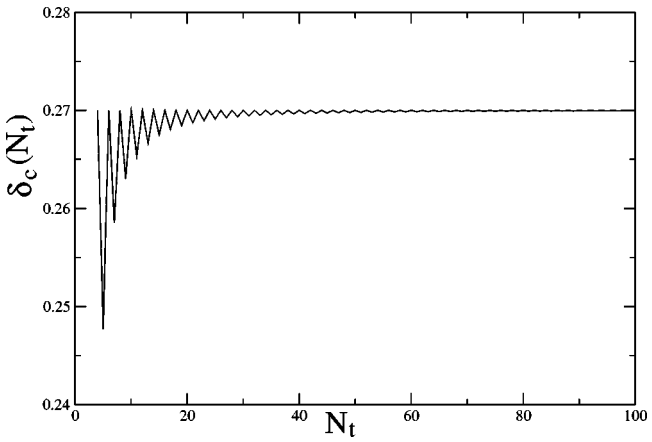

FIG. 1. The dependence of nonstaticity δ_t^*, defined at the bifurcation point for analytic KvB caloron solutions, on the number of time slices, N_t. The zigzag form of the curve can be explained by the qualitatively different arrangement of even and odd time points where the continuum KvB caloron solution has to be calculated in order to evaluate Eq. (3).

If the nonstaticity is lower than the bifurcation value δ_t^*, two dyons can be distinguished by the two maxima of the action density. If the nonstaticity is bigger than δ_t^*, two dyons appear recombined into a caloron with only one action density maximum.

III. RECOMBINATION OF DYONS INTO CALORONS WITH LOWERING TEMPERATURE

The main results of this paper are obtained from ensembles of $SU(2)$ gauge field configurations created by heat bath Monte Carlo simulations at $\beta=2.2$ with respect to the Wilson action S_W on lattices $16^3\times N_t$ with $N_t=4$, $N_t=5$, and $N_t=6$. Each ensemble consisted of about 8000 independent configurations. Cooling of these configurations was performed using the fastest possible relaxation with respect to the Wilson action. For this method each link $U_{x,\mu}$ is immediately replaced by the projection to $SU(2)$ of the staples around it, $\tilde{U}_{x\mu}$.

The cooled configurations studied in this paper have been identified when the cooling history finally has arrived at a quasistable plateau on the level of a single instanton action $S_W\approx S_{inst}=2\pi^2\beta$. Later on, we describe also some results concerning higher plateaus of the action—e.g., $S_W\approx 3S_{inst}$—which are passed earlier in the cooling process. More precisely, on such plateaus we stopped cooling always at local minima of the violation of the lattice equations of motion [6]. Here, the violation is defined as

$$V=\sum_{x\mu}\left(\frac{1}{2}\,\mathrm{tr}[U_{x\mu}-\tilde{U}_{x\mu}]^{\dagger}[U_{x\mu}-\tilde{U}_{x\mu}]\right)^{1/2}. \qquad (4)$$

In addition to that, the following conditions have been imposed for the automatized selection of the classical solutions:

(i) the action fits into the window $0.5<S_W/S_{inst}<1.25$,
(ii) the decrease of action has slowed down to $|\Delta S_W|/S_{inst}<0.05$,
(iii) the violation of the equations of motion should be sufficiently weak, $V<25$.

In most of the cases for which the first and second conditions hold we find a small minimum violation $V<20$. In a few cases there were also local minima with much larger V values, which hardly could be interpreted as extended solutions of the lattice equations of motion. Thus, the third condition was implied in order to select ''good'' solutions. We have varied our stopping criteria[2] and seen that the details of the ensemble of the ''frozen'' objects slightly change. Our main observations reported below do not depend on the details of the procedure. The efficiency of the conditions was such that 80% (in the case $N_t=4$), 60% ($N_t=5$), and 55% ($N_t=6$) of the equilibrium configurations ended up in a cooled configuration at the one-instanton action plateau. These cooled configurations include events with topological charge $Q=\pm 1$—i.e., real calorons—as well as configurations with topological charge $Q=0$ which in our previous paper [6] had been identified as static dyon-antidyon pairs ($D\bar{D}$). The latter constitute 18% ($N_t=4$), 14% ($N_t=5$), and 8% ($N_t=6$), respectively, of all cooled configurations at the one-instanton level. They have been discarded from the considerations in this paper.

We remind the reader that the recombination threshold $\delta_t^*=0.27$, strictly speaking, reflects the recombination for maximally nontrivial holonomy only—i.e., with an asymptotic value of the Polyakov line $L_{as}=0$. If one performs cooling without special restrictions concerning the holonomy, there is no guarantee that the asymptotic holonomy of the caloron configurations still coincides with the average Polyakov line of equilibrium configurations in confinement. For the purpose of defining an *asymptotic* holonomy L_{as} for each cooled configuration, we have determined the average of $L_{\vec{x}}$ over a 3D subvolume where the local 3D action density $s_{\vec{x}}$ is low, for definiteness $s_{\vec{x}}<0.0001$. In Fig. 2 we present the distribution of cooled configurations over L_{as} as a histogram (with bin size 0.1) for the three cases $N_t=4$, $N_t=5$, and $N_t=6$. In the legend we show the respective volume fraction ($F\approx 0.15$) of the three-volume over which the ''asymptotic'' value L_{as} is defined as an average—i.e., far from the lumps of action and topological charge.

As explained above, the nonstaticity δ_t is a measure which describes the distance from a perfectly (Euclidean) time-independent configuration. In other words, the distributions of nonstaticity of caloron events obtained by cooling of equilibrium lattice configurations can be considered as a substitute for the distribution in dyon distances d. This quantity can be directly measured for cooled lattice gauge field configurations. We show in Fig. 3 the δ_t distributions for all our cooling products obtained at $\beta=2.2$ on $16^3\times N_t$ lattices.

In an attempt to make a fair comparison with calorons with nontrivial holonomy and to correct for the possible evo-

[2]The criteria have been tested for $N_t=4$ and applied also to $N_t=5$ and 6 (at the same β).

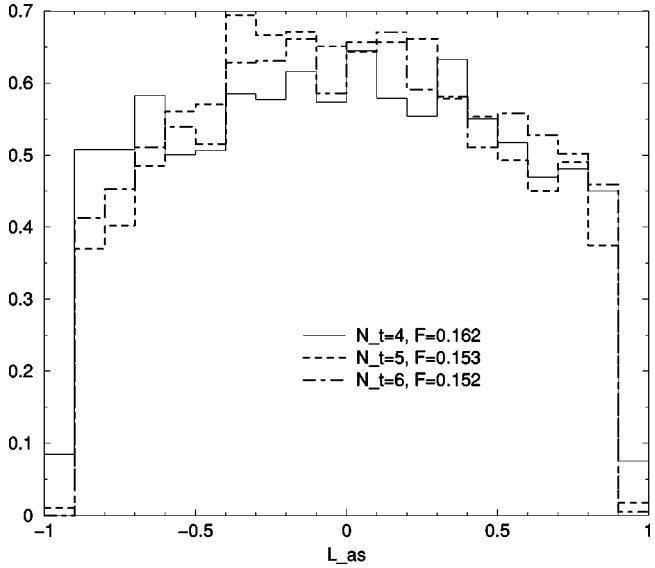

FIG. 2. The distribution of holonomy L_{as} for the three samples of cooled configurations corresponding to three temperatures below deconfinement at $N_t=4$, $N_t=5$, and $N_t=6$.

lution of the asymptotic holonomy away from $L_{as}=0$ during the cooling process, we defined a subsample by the requirement $|L_{as}|<1/6$. One can see that the cut with respect to the asymptotic holonomy selects cooled configurations from the flat central part of the histogram shown in Fig. 2. On the other hand, we notice that a considerable fraction of cooled configurations has developed an asymptotic holonomy $|L_{as}|>1/6$.

In Fig. 3(a) we show the probability distribution over δ_t for cooled configurations with an action at the one-instanton plateau without the cut according to the asymptotic holonomy $|L_{as}|$. One can see that a relatively high fraction of configurations, obtained from the Monte Carlo equilibrium with $N_t=4$, has $\delta_t<\delta_t^*=0.27$. This means that they would be identifiable as consisting of two constituents by looking for the 3D action density on the lattice. For $N_t=5$ it is only a minority of cooled configurations which falls below the threshold $\delta_t=0.27$. No static (according to the nonstaticity criterion) configurations have been found among cooling products at $N_t=6$.

We have repeated the same analysis after applying the cut with respect to the asymptotic holonomy, $|L_{as}|<1/6$. Then we get modified histograms in δ_t for the three temperatures. This is shown in Fig. 3(b). The histograms got more pronounced peaks in δ_t which are positioned around 0.125, exactly around $\delta_t^*=0.27$, and around 0.5 for $N_t=4$, $N_t=5$, and $N_t=6$, respectively.

There are other criteria which could be used to characterize a more or less static configuration—for example, the presence of static Abelian monopoles emerging in the maximal Abelian projection. This criterion is not identical with the separation set by δ_t^*. Thus, another subsample can be defined by the property that a pair of static Abelian monopoles has been found after fixing the cooled configuration to the maximal Abelian gauge and doing the Abelian projection. This subsample can be analyzed with respect to the three-dimensional distance R between the Abelian monopoles.

In Fig. 4(a) we show the histogram over δ_t of all cooled configurations obtained from the Monte Carlo ensemble at $N_t=4$ together with the histogram of those which explicitely exhibit the dyon-dyon structure in terms of Abelian monopoles. One can see that practically all cooled configurations below δ_t^* possess this structure, but above δ_t^* the fraction rapidly goes to zero. We show the same for $N_t=6$—i.e., at lower temperature—in Fig. 4(b). In this case, at the peak value around $\delta_t=0.5$ only 20% of the solutions still are characterized by a static dyon-dyon pair, whereas at higher nonstaticity this is never the case. In these two distributions no cut with respect to the asymptotic holonomy has been applied.

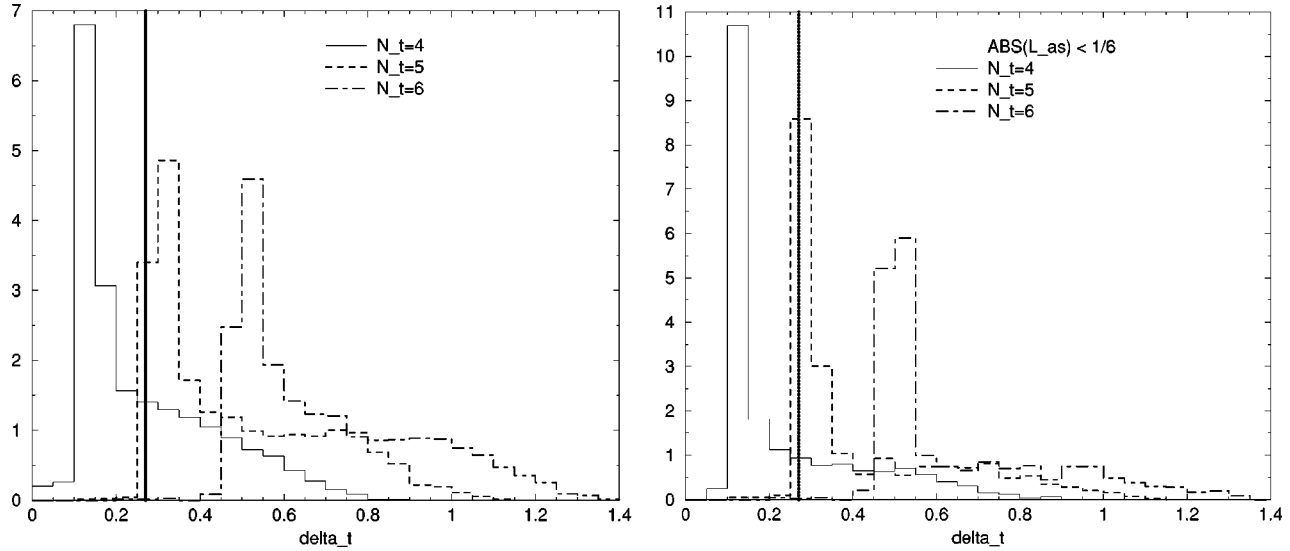

FIG. 3. The distribution of nonstaticity δ_t after cooling as histograms (with bin width 0.05), for three temperatures below deconfinement at $N_t=4$, $N_t=5$, and $N_t=6$: (a) without any cut, (b) when a cut $|L_{as}|<1/6$ is applied. The thick vertical line marks the nonstaticity δ_t^* where the caloron recombines.

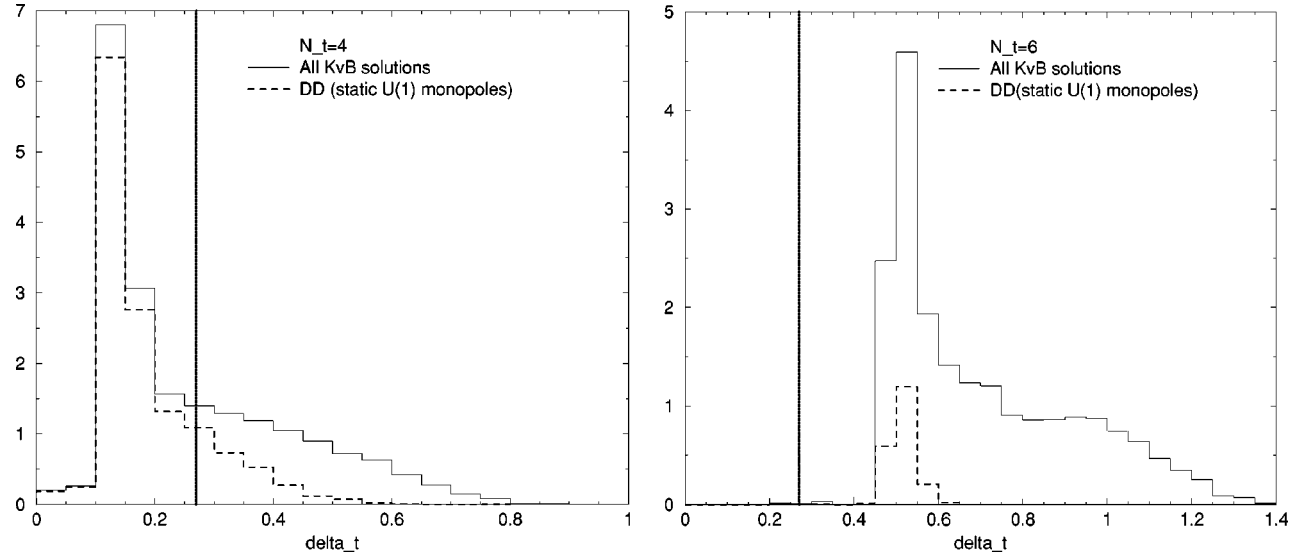

FIG. 4. The distribution of nonstaticity δ_t after cooling compared with the subsample of configurations which have a static dyon-dyon (DD) structure exhibited by monopoles after Abelian projection: (a) for the higher temperature with $N_t=4$, (b) for the lower temperature with $N_t=6$. The thick vertical line marks the nonstaticity δ_t^* where the caloron recombines.

Up to now we have two tentative definitions of the position of the constituents: one is the position of the two static Abelian monopoles (in MAG, as long as they are static) and the other is defined by the maxima of the 3D action density.[3] In the case of well-separable maxima of the latter these maxima fall close to the positions of the MAG monopoles. In the other limiting cases of recombined maxima or imbalanced maxima (this corresponds to an asymptotic holonomy far from zero) of the 3D action density at least the *absolute maximum of action density* is still easy to find. It is either *the* single maximum or it takes the role of *one* of the maxima. For the case of $N_t=4$—i.e., the temperature just below deconfinement—we show in Fig. 5(a) the histogram with respect to the local Polyakov loop at the two sorts of 3D constituent points: the loci of static monopoles or the maximum of action density. In both definitions the histogram peaks near to $L_{\vec{x}}=\pm 1$. The peak is, however, more pronounced for the monopole locations, less pronounced for the maxima of the 3D action density.

The relation between the nonstaticity δ_t and the distance R between the static dyonic constituents emerging (in MAG as Abelian monopole) given in lattice units is presented in Fig. 5(b) for the higher temperature, near the deconfinement temperature $(N_t=4)$. For this temperature such dyon-dyon events are clearly distinguishable among the cooled configurations as long as the nonstaticity $\delta_t<0.6$. For extremely low nonstaticity δ_t [left from the peaks in Figs. 3(a) and 3(b)] we find an average distance $R\approx 7$, whereas near δ_t^* the average distance is $R\approx 4$. For higher δ_t, the part of solutions which still possesses a clear dyon-dyon structure in terms of Abelian monopoles has them localized at distances R between one and two lattice spacings.

In order to represent how the Polyakov line behaves inside a lump of action, we have chosen the absolute maximum of the 3D action density (denoted as central point $\vec{x}_0$) and have explored the Polyakov loop in its neighborhood. For this purpose, we have defined a locally summed-up Polyakov line L_{tot} [summed over the central point $\vec{x}_0$ and its six nearest neighbors $\vec{x}_i (i=1,\ldots,6)$],

$$L_{tot}=\sum_{i=0}^{6} L_{\vec{x}_i}, \tag{5}$$

and a kind of Polyakov-line dipole moment over the same set of 3D lattice points with respect to the central point:

$$\vec{M}_{tot}=\sum_{i=1}^{6} L_{\vec{x}_i}(\vec{x}_i-\vec{x}_0). \tag{6}$$

The absolute value $|L_{tot}|$ of the first quantity tests the amount of local coherence of the Polyakov line. The absolute value $|\vec{M}_{tot}|$ of the second quantity tests the amount of presence of opposite-sign Polyakov lines representing eventually two different constituents inside the same lump of action. Figure 6(a) shows how the $|L_{tot}|$ (i.e., the locally summed-up Polyakov line) changes with δ_t in different bins of width 0.1. For the temperature nearest to the transition, at $N_t=4$, we see that $|L_{tot}|$ falls from ≈ 4.0 to ≈ 1.0 at $\delta_t \geqslant 0.5$. We interprete this such that in the region, where constituents can be well separated according to the action density (at small δ_t), they are characterized by a relatively smooth change of the Polyakov line inside. In the region of large δ_t where they are not separable according to the action density, the Polyakov line changes rapidly in the neighborhood of the absolute maxi-

[3]For the case of analytical caloron solutions, the relation between the constituent locations, the locations of the maxima of the action density and the locations where $|P|=1$ has been compared in Ref. [16].

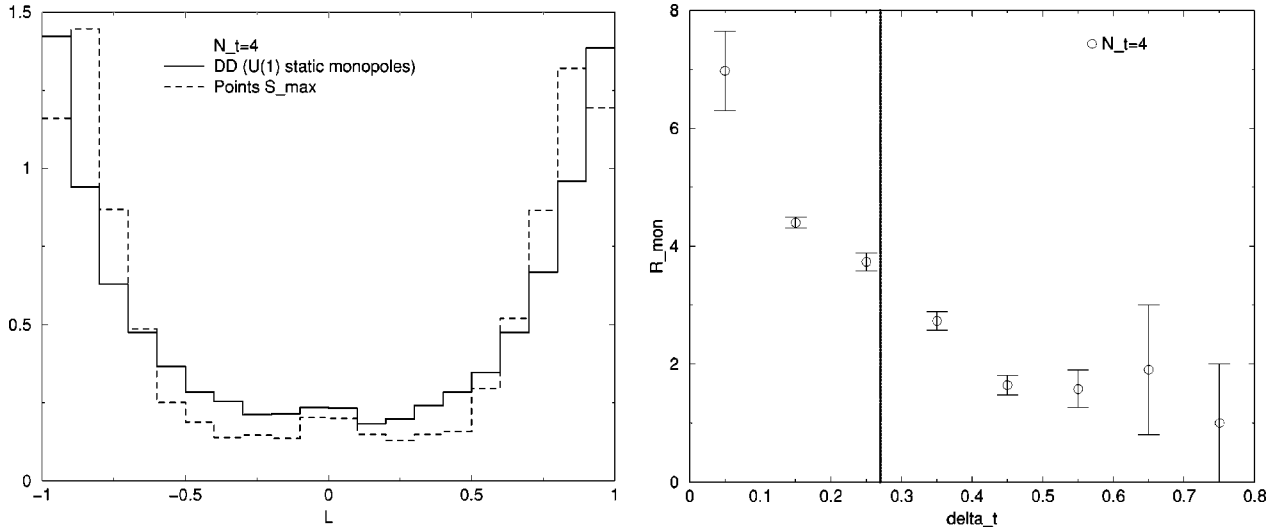

FIG. 5. The dyon-dyon structure after Abelian projection: (a) distribution of the local Polyakov loop at the position of the static Abelian monopoles compared to the distribution at the maxima of action density, (b) average distance between the static Abelian monopoles vs nonstaticity δ_t assigned to the cooled configuration. The thick vertical line marks the nonstaticity δ_t^* where the caloron recombines.

mum of action density. For the lower temperatures $N_t=5$ and $N_t=6$, the relationship between these properties of an action cluster and δ_t is the same. The difference is that separable lumps of action (those with low δ_t) become very rare. Figure 6(b) shows how the ''dipole moment'' $|\vec{M}_{tot}|$ of the Polyakov line around a maximum of action density rises with increasing nonstaticity δ_t. In the region where one can separate the constituents according to the action density, the dipole moment is small, emphasizing again the homogeneity of the Polyakov line around the central point. In the region beyond δ_t^* the dipole moment gradually stabilizes around a value of 1.5.

In the same way as described so far, we have analyzed configurations obtained by cooling at higher-action plateaus. As an example we show in Fig. 7 the histogram of nonstaticity δ_t for the same three temperatures represented by $N_t=4$, $N_t=5$, and $N_t=6$. Although the precise border between static and nonstatic has not the clear meaning as for the one-caloron case, the trend is the same: at lower temperature the lumps of action tend to be more localized also in Euclidean time (''instanton like''). Compared with the one-caloron case, the histograms are more smeared.

So far we have investigated the outcome from cooling for varying temporal lattice extent and fixed spatial volume. What happens when changing β at fixed lattice size and fixed lattice asymmetry? In Fig. 8 we again show nonstaticity δ_t histograms without applying cuts for $|L_{as}|$. We compare (a) for $N_t=4$ the cases $\beta=0$, $\beta=2.04$, and $\beta=2.20$

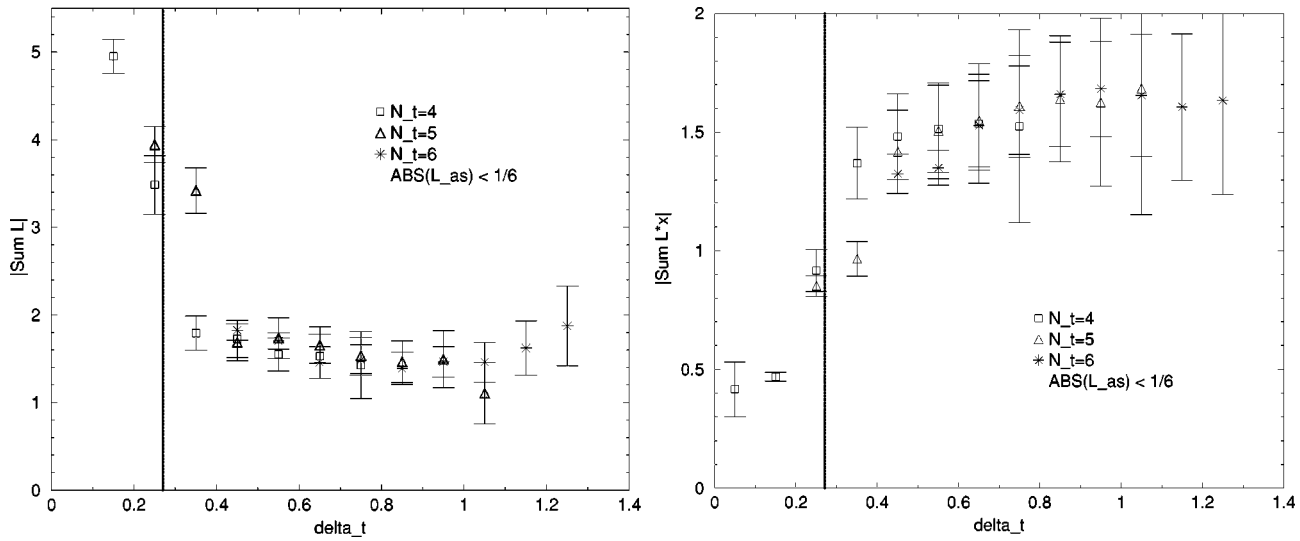

FIG. 6. The Polyakov line in the neighborhood of maxima of the action density: (a) modulus of the average summed-up Polyakov line $|L_{tot}|$, (b) modulus of the corresponding ''dipole moment'' $|\vec{M}_{tot}|$ vs nonstaticity δ_t, for the subsample with asymptotic holonomy near zero. For details of the definition see the text. The thick vertical line marks the nonstaticity δ_t^* where the caloron recombines.

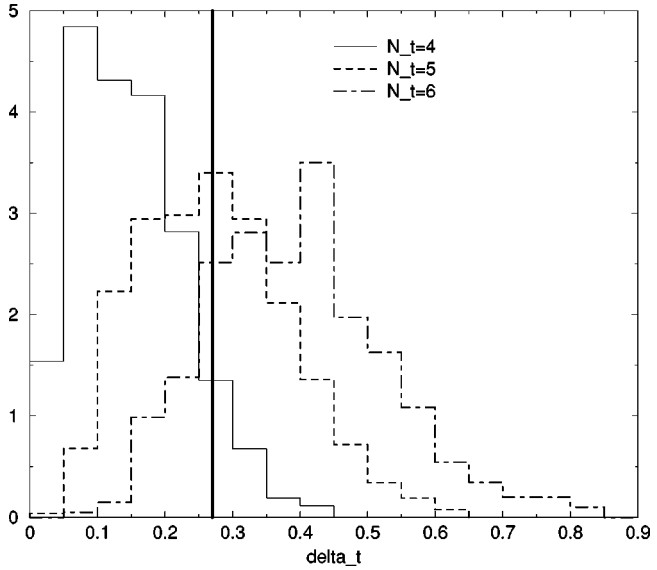

FIG. 7. The same as in Fig. 3(a) for $S=3S_{inst}$ plateaus. No cut in the asymptotic holonomy has been applied. The thick vertical line marks the nonstaticity δ_t^* where the caloron recombines.

with each other and (b) for $N_t=6$ the case $\beta=2.20$ with $\beta=2.36$.[4] The statistics for the new β values (0.0, 2.04 and 2.36) is of order $O(200)$ field configurations each. Contrary to what one might have expected, we see that among the cases (a) and (b), respectively, there are no qualitative differences. This means that the ratio of probabilities for the occurrence of dissociated calorons (or separate static dyon pairs) versus nondissociated (single lump) calorons is *not* a function of the temperature describing the original equilibrium ensemble. Instead, it is mainly determined by the geometry (the aspect ratio) of the lattice. The larger the temporal lattice extent is in comparison with the spatial extent, the lower is the probability to find separated lumps of more or less static objects after cooling. In other words, once there is only one topological $Q\neq 0$ object left, everything is classical. As a rule, the object is smooth, such that only the size of the box matters or other ''infrared forces'' (e.g., those forbidding single instantons) play a role. This observation clearly shows the limitation of the cooling method applied to the lowest-action plateaus.

IV. INSTANTONS OR CALORONS ON A SYMMETRIC 4-TORUS

With low statistics (100 configurations) we have also cooled equilibrium configurations generated with $\beta=2.2$ on symmetric lattices (16^4 representing ''zero'' temperature). In this case we have found for the classical configurations at the plateau $S_W\approx S_{inst}$ a broad distribution of nonstaticity with a maximum around $\delta_t\approx 2$ and with a tail extending beyond 3 (see Fig. 9). These are obviously configurations with an action (topological charge) density well localized in all four Euclidean directions. There is a nontrivial behavior of the Polyakov line inside these nondissociated, instantonlike objects resembling the Polyakov line associated with the time direction in the finite-temperature case for nondissociated calorons. We have mapped the cooled lattice configuration with the help of all four possible definitions of the Polyakov line, which are now, on a symmetric lattice, physically equivalent to each other. Figure 10 shows the profiles of the action density, topological charge density, and the Polyakov lines (for four possible definitions) as they are seen in appropriate planes intersecting the lump through the centrum. The latter is defined as the maximum of the 4D action density. For all types of Polyakov lines the characteristic double structure is seen exactly when the ''asymptotic'' value of the respective Polyakov line is *not close* to ± 1.

It is interesting to compare the pattern of the Polyakov line of these ''caloron candidates'' with the analytic KvB caloron formally constructed on a 16^4 lattice corresponding to maximally nontrivial holonomy with respect to what has been chosen as the ''time'' direction. For this construction, the two constituents have been placed along the z direction, separated by eight lattice spacings. The lattice caloron is obtained calculating link by link from the continuum gauge field A_μ. Of course, such a constructed lattice caloron has irregularities at the boundary if the lattice action is evaluated under the assumption of periodicity. After some cooling the configuration turns into an (approximate) solution of the lattice equations of motion *on the torus*. By that time the boundary artifacts have disappeared (see Fig. 11), and the Wilson action has become $S_{inst}=2\pi^2\beta$. The KvB caloron is now adjusted to periodic boundary condition also in the x,y,z directions. Despite the large separation the constituents formally have, judging according to the action density it is a nondissociated caloron. It is seen that the cooling does not influence significantly the structure of the Polyakov lines of the KvB caloron witnessed by the time-directed Polyakov line (*plt*) showing the double-peak structure mentioned above. The space-directed Polyakov lines (plx,ply,plz) have a simple structure characteristic for trivial holonomy. It is analytically clear that for caloron solutions asymptotically $plx,ply,plz\rightarrow\pm 1$. This is in contrast to the would-be ''caloron candidate'' obtained by cooling from confining equilibrium lattice configurations at zero temperature (Fig. 10) where the double-peak structure is present for all t,x,y,z directions and, generically, the asymptotic holonomy in all directions is nontrivial.

V. CONCLUSIONS AND PERSPECTIVES

In the present investigation we have subjected equilibrium lattice gauge fields corresponding to various temperatures to ordinary relaxation (usually called ''cooling'') in order to obtain an ensemble of classical solutions for further study. In this way we have extracted lowest-action classical solutions of unit topological charge typical for the given equilibrium ensemble. Notice that, at least as long this technique is used, this possibility is restricted to the confinement phase. We do not claim to find the real and complete topological structure

[4]Note that according to asymptotic scaling ($\beta=2.20$, $N_t=4$) and ($\beta=2.36$, $N_t=6$) would correspond approximately to the same physical temperature.

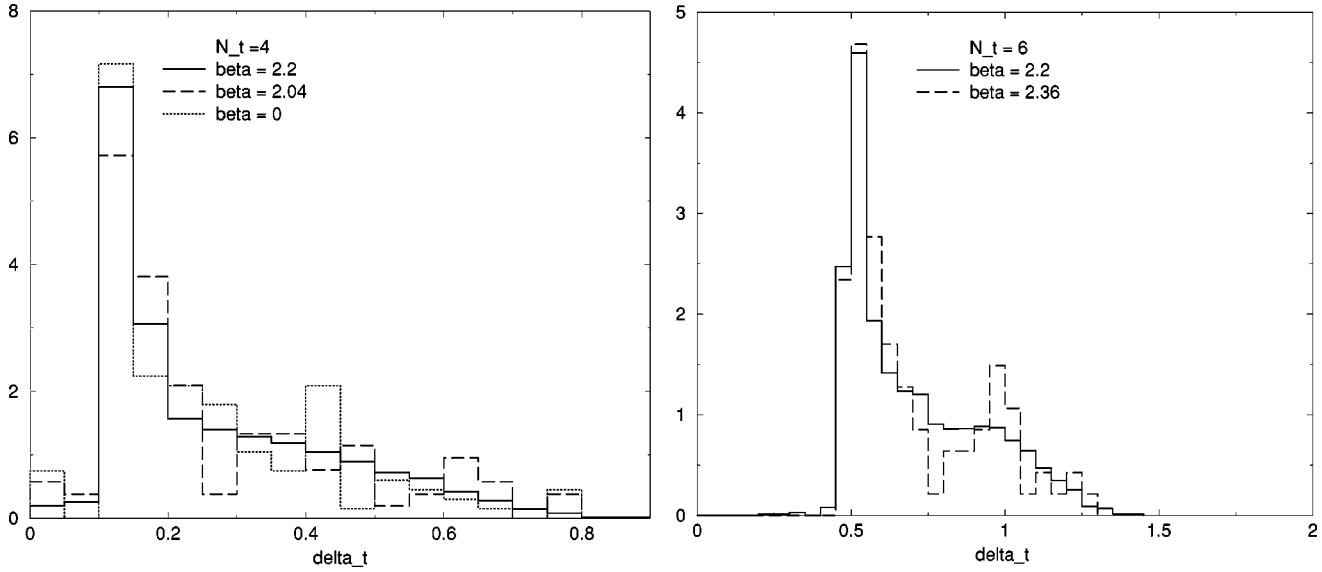

FIG. 8. The distribution of nonstaticity δ_t after cooling for fixed N_t but varying β values. No cut in the asymptotic holonomy is made. The spatial lattice size is always 16^3. (a) $N_t=4$: $\beta=0.0$, 2.04, 2.20. (b) $N_t=6$: $\beta=2.20$, 2.36.

hidden under the quantum fluctuations and consisting of topological lumps of compensating sign. What we wanted to see were the simplest solutions suitable as building blocks for a semiclassical modelling of the Yang-Mills path integral. In conclusion we can say that cooling of equilibrium lattice fields in $SU(2)$ lattice gauge theory shows that there exist topological objects with a dyonic substructure and that we are able to resolve only in the confined phase. With increasing temporal lattice extent it becomes more probable that the observed dyons recombine into calorons such that it becomes impossible to perceive the substructure looking *exclusively* at the distribution of action and topological charge. Strictly speaking, we have found that the fraction of dissociated calorons among all single-calorons events does not depend on the physical temperature of the equilibrium fields but on the geometric aspect ratio of the box—i.e., the asymmetry of the lattice. However, all calorons have a nontrivial holonomy which is mapped out by the behavior of the Polyakov line *inside and outside* these configurations.

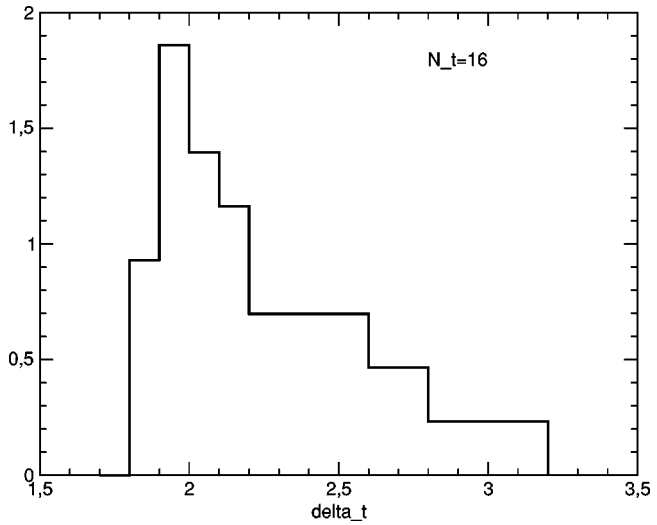

FIG. 9. The distribution of nonstaticity δ_t after cooling for $\beta=2.2$ on the symmetric lattice 16^4, obtained from 42 configurations with unit topological charge.

In the limiting case of zero temperature (i.e., on a symmetric lattice) topological lumps with $Q=\pm 1$ obtained by cooling look instanton like and, at the same time, have the characteristic double-peak structure of the Polyakov line in *all* t,x,y,z directions. This distinguishes them from the real KvB solutions which possess this structure only with respect to a distinguished ''time'' direction.

Strictly speaking, an analytic solution of the Euclidean equations of motion with $Q=\pm 1$ is impossible on the 4D torus [9]. Nevertheless, on the lattice quasistable solutions of this kind exist. If considered only as lumps of action and topological charge, there is no contradiction with the previous observations from ''instanton searches.'' As our analysis shows, for temperatures much lower than the deconfinement temperature rotationally symmetric (in 4D) and (anti-)self-dual lumps seem to be preferred under cooling.

At finite temperature, they can be subsumed under the general class of KvB solutions. For zero temperature, however, a so-far unknown parametrization with nontrivial asymptotic holonomy has yet to be found.

After having completed the present investigation we were informed by Gattringer and Pullirsch [15] about their paper ''Topological lumps and Dirac zero modes in $SU(3)$ lattice gauge theory on the torus'' prior to publication. In this paper the authors concentrate on and more systematically continue the inspection of the low-lying modes of the chirally improved Dirac operator on the 4-torus, in the background of equilibrium lattice gauge fields at $T=0$. It is extremely interesting that they find, for a certain fraction of Monte Carlo configurations in the $|Q|=1$ sector, a similar pattern of hopping zero modes as a function of varying fermionic boundary conditions as for $T\neq 0$. Moreover, the change of localization

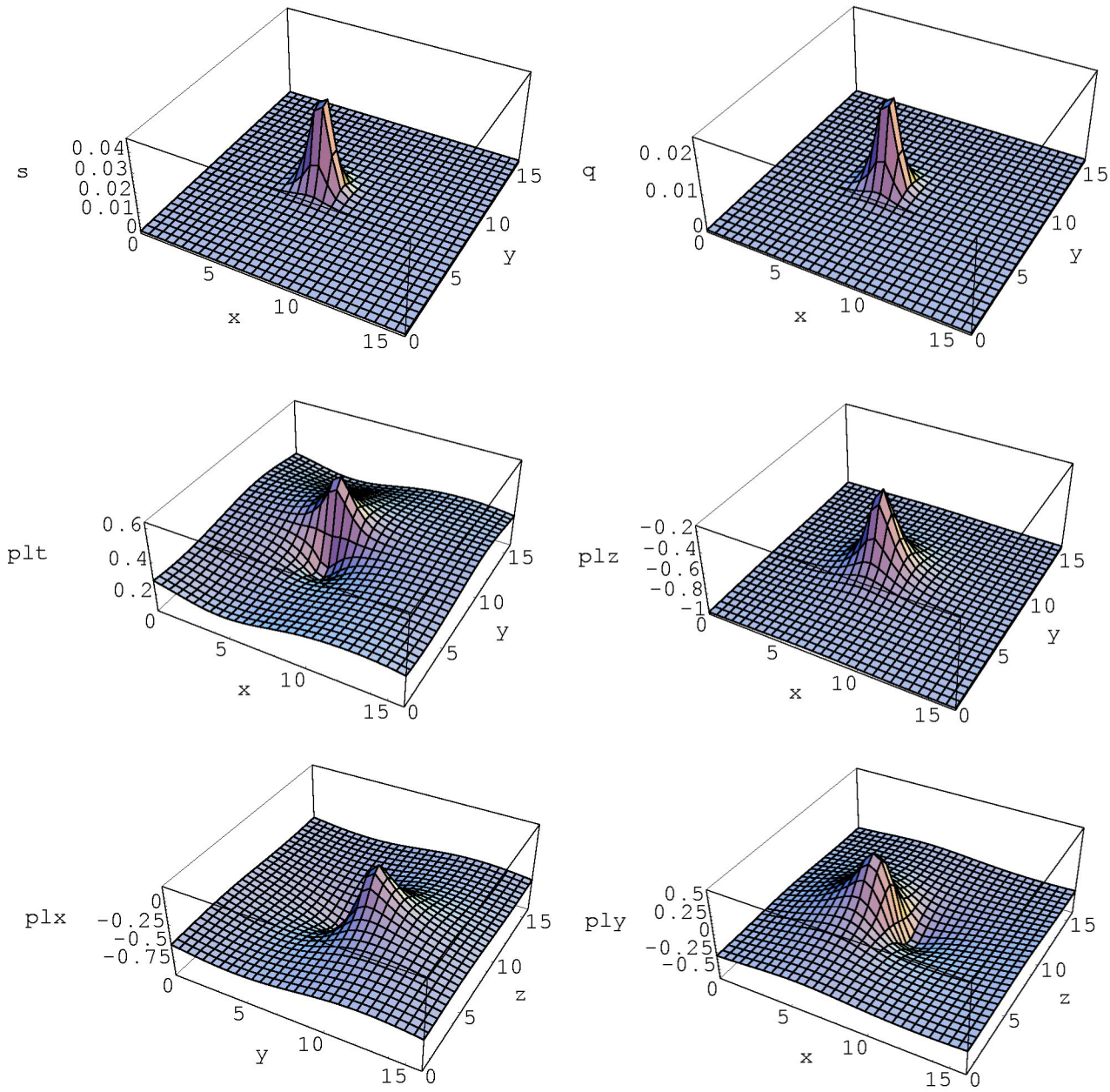

FIG. 10. Profiles of the action density (s), the topological charge density (q), and the Polyakov lines (plt,plx,ply,plz) calculated along all straight line pathes parallel to the four axes for a 16^4 lattice caloron found by cooling a Monte Carlo—generated equilibrium gauge field down to the one-instanton action plateau. The center of the caloron (at the maximum of its action density) was found at the site $(x,y,z,t)=(7,8,8,14)$. The planes shown in the figures cross just this point.

happens independently of which of the four directions is chosen as the ''imaginary time'' direction along which periodicity can be purposedly changed. The concurrent zero-mode positions (two or three as in the finite-temperature case) are consistent with being randomly distributed in the 4D periodic box. The authors argue that this observation hints at the existence of a semiclassical background consisting of localized (in 4D) instanton constituents. Whereas other (monopole?) properties of the constituents are less obvious, a noninteger topological charge of the constituents has been hypothetically assumed in analogy with the dissociated KvB solutions. In fact, this should not be too difficult to be established. It is in particular this last interpretation that has to pass further tests. In case it becomes confirmed then it would be difficult to reconcile this with our observations based on cooling. Our findings are consistent with a picture in which (at finite temperature) the temporal size of the box determines (inversely) the size of the background solutions. In contrast, the scenario of Ref. [15] seems to imply a complete dissolution (within the available 4-volume) of some constituents which still span a coherent semiclassical background. This would mean that there is no scale of coherence which is dynamically generated and decoupled from the overall size of the box. If the latter picture can be confirmed, we would

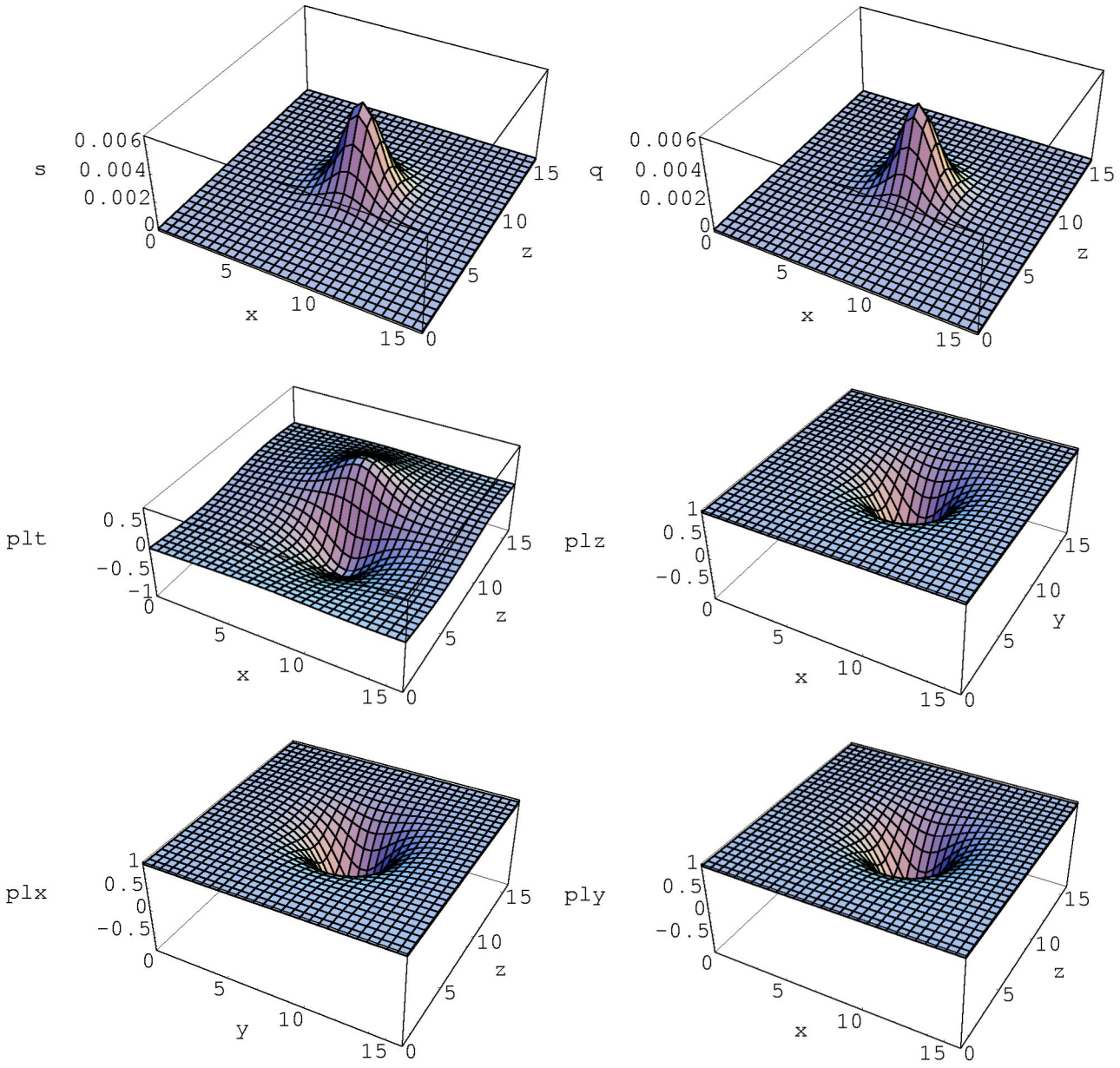

FIG. 11. Profiles of the action density (s), the topological charge density (q), and the Polyakov lines (plt,plx,ply,plz) as in Fig. 10 but for a 16^4 lattice caloron obtained from a discretized KvB solution corrected by some cooling to the one-instanton action plateau (309 cooling steps). The center of the caloron (at the maximum of its action density) was placed to the site $(x,y,z,t)=(8,8,8,1)$. The planes shown in the figures cross this point.

have to blame cooling (or the cooling action we have used) for artificially driving all semiclassical configurations into integer-charged topological lumps at lower temperatures whereas separated monopole constituents are correctly reproduced by cooling only at higher temperatures. This would explain why previous studies of the topological properties using various cooling (smoothing) techniques (which actually missed the relevant temperature range) were not suitable to discover the nontrivial holonomy accompanying all topological charges.

There is still an ongoing debate on the question in as far a semiclassical interpretation of the QCD vacuum is valid at all [17]. For the time being we have nothing to add to this discussion. But our results point to the fact that the instanton gas or liquid model (as well as other models) have to be reconsidered by taking into account the nontrivial holonomy structure. We believe that this will improve the bad performance of (trivial holonomy) instantons in comparison with lattice smoothing results as reported in [18,19].

ACKNOWLEDGMENT

Three of us (E.-M.I., B.V.M., and M.M.-P.) gratefully acknowledge the kind hospitality extended to them at the Instituut-Lorentz of the Universiteit Leiden, where this paper

became finalized. We thank Pierre van Baal, Falk Bruckmann, and Christof Gattringer for useful discussions and e-mail correspondence in the final stage of the work. This work was partly supported by RFBR grants 02-02-17308, 03-02-19491, and 04-02-16079, DFG grant 436 RUS 113/739/0, and RFBR-DFG grant 03-02-04016, and by Federal Program of the Russian Ministry of Industry, Science and Technology No 40.052.1.1.1112. Two of us (B.V.M. and A.I.V.) gratefully appreciate the support of Humboldt-University Berlin where this work was initiated and carried out to a large extent. The work of E.-M.I. at Humboldt-University is supported by DFG (FOR 465).

[1] T.C. Kraan and P. van Baal, Phys. Lett. B **435**, 389 (1998).
[2] T.C. Kraan and P. van Baal, Nucl. Phys. **B533**, 627 (1998).
[3] E.-M. Ilgenfritz, M. Müller-Preussker, and A. I. Veselov, in Proceedings of the NATO Advanced Research Workshop on Lattice Fermions and Structure of the Vacuum, Dubna, Russia, 1999, edited by V. K. Mitrjushkin and G. Schierholz, NATO ASI Series C, Vol. 553 (Kluwer Academic, Dordrecht, 2000), p. 345.
[4] E.-M. Ilgenfritz, B.V. Martemyanov, M. Müller-Preussker, and A.I. Veselov, Nucl. Phys. B (Proc. Suppl.) **94**, 407 (2001).
[5] E.-M. Ilgenfritz, B.V. Martemyanov, M. Müller-Preussker, and A.I. Veselov, Nucl. Phys. B (Proc. Suppl.) **106&107**, 589 (2002).
[6] E.-M. Ilgenfritz, B.V. Martemyanov, M. Müller-Preussker, S. Shcheredin, and A.I. Veselov, Phys. Rev. D **66**, 074503 (2002).
[7] C. Gattringer, Phys. Rev. D **67**, 034507 (2003); C. Gattringer and S. Schaefer, Nucl. Phys. **B654**, 30 (2003).
[8] C. Gattringer, E.-M. Ilgenfritz, B.V. Martemyanov, M. Müller-Preussker, D. Peschka, R. Pullirsch, S. Schaefer, and A. Schäfer, Nucl. Phys. B (Proc. Suppl.) **129&130**, 653 (2004).
[9] P.J. Braam and P. van Baal, Commun. Math. Phys. **122**, 267 (1989).
[10] H.D. Trottier and R.M. Woloshyn, Phys. Rev. D **50**, 6939 (1994); R.M. Woloshyn and F.X. Lee, *ibid.* **53**, 1709 (1996).
[11] G. 't Hooft, Phys. Rev. D **14**, 3432 (1976); C.G. Callan, R.F. Dashen, and D.J. Gross, *ibid.* **17**, 2717 (1978); D.J. Gross, R.D. Pisarski, and L.G. Yaffe, Rev. Mod. Phys. **53**, 43 (1981); E.-M. Ilgenfritz and M. Müller-Preussker, Nucl. Phys. **B184**, 443 (1981); E.V. Shuryak, *ibid.* **B203**, 93 (1982); **B203**, 116 (1982); **B203**, 140 (1982); D.I. Dyakonov and V.Yu. Petrov, *ibid.* **B245**, 259 (1984).
[12] For recent reviews see E.V. Shuryak and T. Schäfer, Rev. Mod. Phys. **70**, 323 (1998); D.I. Dyakonov, Prog. Part. Nucl. Phys. **51**, 173 (2003).
[13] A.A. Belavin, A.M. Polyakov, A.S. Schwartz, and Yu.S. Tyupkin, Phys. Lett. **59B**, 85 (1975).
[14] B. Harrington and H. Shepard, Phys. Rev. D **17**, 2122 (1978).
[15] C. Gattringer and R. Pullirsch, Phys. Rev. D **69**, 094510 (2004).
[16] M. Garcia Perez, A. Gonzalez-Arroyo, A. Montero, and P. van Baal, J. High Energy Phys. **06**, 001 (1999).
[17] I. Horvath *et al.*, Phys. Rev. D **66**, 034501 (2002); **67**, 011501 (2003).
[18] T.G. Kovacs, Phys. Rev. D **62**, 034502 (2000).
[19] T. De Grand and A. Hasenfratz, Suppl. Prog. Theor. Phys. **131**, 573 (1998).